JOURNAL OF MATERIALS SCIENCE 31 (1996) 2139–2143

Microstructural characterization of a rapidly-solidified Al–12 wt % Si alloy

YÜCEL BIROL
Materials Research Division, Marmara Research Center, Tübitak, Gebze, Kocaeli, Turkey

Optical, electron metallography and X-ray diffraction techniques were employed to characterize the microstructure of a rapidly solidified Al–12 wt % Si alloy. Ribbons produced with the planar flow casting process at a cooling rate of 10^6 K s^{-1}, had a very fine cellular structure of αAl and nanosize Si particles which are distributed inside and at the boundaries of these cells. Thinner sections ($t < 30$ μm) have apparently experienced higher cooling rates and show, in addition to a cellular structure, a distinct zone which is featureless at optical microscope magnifications.

1. Introduction

Increasing demand for high performance materials calls for constitutional as well as microstructural modification of those alloys which are currently available in the market and also requires development of novel alloy compositions with better properties. It is well established that rapid solidification processing (RSP) offers some distinct advantages over conventional ingot metallurgy in this regard [1, 2].

Among several metals for which RSP methods have been put to use, aluminium has been the most fortunate. The equilibrium solid solubility of many elements in aluminium is very limited in contrast to that in the liquid state where they enjoy a nearly perfect miscibility. Thus, the aluminium system, with many potentially useful alloying additions from the periodic table [3], takes full advantage of the large deviations from equilibrium encountered in RSP. Some of the unique features achieved through rapid solidification of aluminium alloys include, in order of increasing solidification rates [4, 5],

(i) a refined microstructure (very small grain size and fine precipitates),
(ii) increased chemical homogeneity (reduced segregation, uniform distribution of 2nd phase particles),
(iii) extension of solid solubility (orders of magnitude in some cases),
(iv) formation of metastable (crystalline, quasicrystalline, amorphous) phases.

Much of the attention in rapid solidification studies of aluminium alloys has been directed to improving the properties of aerospace alloys [6, 7]. Alloys for automotive applications, on the other hand, have received less attention due to the high cost of RSP which cannot be justified on the basis of performance alone. One exception has been Al–Si alloys [8–18] which are widely used in automotive industries as a basic foundry alloy owing to their excellent castability and weldability.

In the present work, ribbons of an Al–12 wt % Si alloy were rapidly solidified by the planar flow casting (PFC) technique. The microstructure of these ribbons were characterized and compared with those of conventionally cast material of the same composition.

2. Experimental

The aluminium alloy used in this investigation was supplied by Seydisehir aluminium works of Etibank in as-cast condition. Its nominal composition conformed to that of the commercial alloy: AA 413 (Al–12 wt % Si).

The as-received material was remelted in a graphite crucible, internally coated with boron nitride and spun into ribbons by the PFC process. The PFC was performed in air using a copper-beryllium wheel, 40 cm in diameter. The molten alloy was ejected from the crucible under an argon pressure of approximately 0.2 kg cm^{-2}, shortly after melting was completed. The temperature of the melt at the onset of ejection was estimated to be 50 °C above the liquidus temperature.

The ribbons thus produced, were 10–15 mm wide, continuous but of poor quality with many pinholes along their length. The thickness was reasonably uniform in the 40–50 μm range, but was reduced to as low as 15 μm in some regions. Such thin regions were grouped separately after a very careful assessment of their thickness following each PFC run.

X-ray diffraction (XRD), light, scanning and transmission electron microscopy (SEM and TEM) techniques were employed to characterize the microstructure of the as-quenched ribbons. The XRD patterns of both the wheel and the air-side of the ribbons were obtained using Cu$K\alpha$ radiation. Specimens for metallographic work were prepared with standard methods and were etched in a 0.5% HF solution. SEM micrographs were taken at an accelerating voltage of 20 KV after these specimens were coated with a

0022–2461

vacuum-deposited gold layer in order to enhance contrast.

Pieces of the ribbons were electropolished in a 10% perchloric acid–90% methanol solution in order to prepare thin foils for TEM. Prior to electropolishing, dimples were ground on either side of these ribbons to obtain thinned regions on the particular side of interest.

3. Results and discussion

The microstructure of the as-received, conventionally-cast alloy (Fig. 1) contains a uniform distribution of eutectic silicon. A few large, faceted crystals of primary silicon can also be identified indicating that the composition is slightly hyper-eutectic. The XRD analysis revealed no intermetallics but only two phases: αAl and Si.

The XRD analysis of the as-quenched ribbons was carried out on both surfaces in order to investigate the cooling effect of the substrate. One set of patterns taken from opposite surfaces of a 45 ± 3 μm thick ribbon is illustrated in Fig. 2. The identical nature of the two patterns implies that a 45 μm ribbon is structurally uniform throughout its thickness.

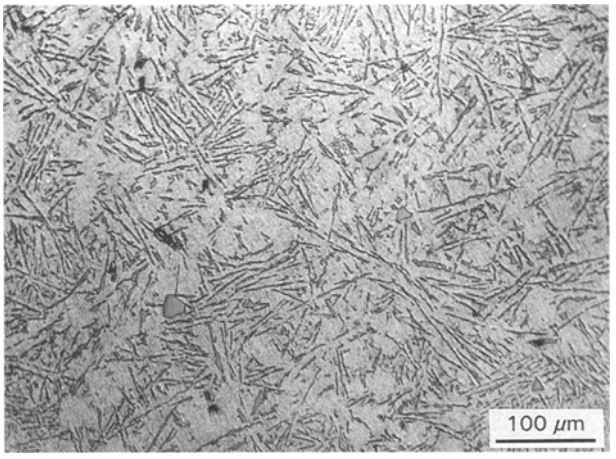

Figure 1 Microstructure of as-received alloy.

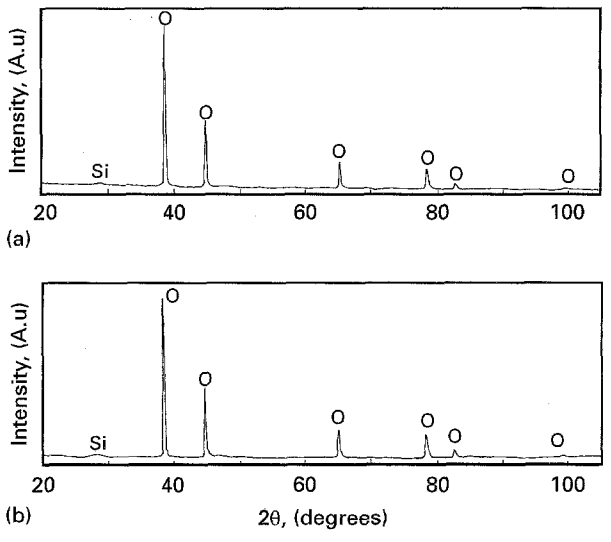

Figure 2 XRD patterns obtained from opposite surfaces of an as-quenched ribbon. (a) Wheel-side, (b) air-side. O: αAl.

In the 2θ range from 20–105 degrees, one can see all the possible reflections of the aluminium solid solution while only a very weak and broad (111) reflection of Si can be identified. This suggests that a substantial amount of the Si is retained in the solid solution as evidenced by the shift of the αAl lines to larger 2θ values.

In order to determine the amount of Si retained in the solid solution upon rapid quenching, the lattice parameter of αAl was calculated and compared with that of the conventionally-cast alloy. A Nelson–Riley extrapolation function was used to calculate the lattice parameters and a shift of 7.31×10^{-4} nm was estimated.

The variation of the αAl lattice parameter with extension of Si solid solubility in Al–Si alloys has been addressed by several investigators [8, 9, 19, 20]. Reported values of lattice parameter change, Δa, range from 3.7×10^{-5} nm [8] to 1.9×10^{-4} nm [9] per at % Si retained in solution. Accordingly, the amount of Si in solution must be somewhere between 19.76 at % and 3.85 at % in the present work. The former value is not realistic, however, considering the chemical composition of the present alloy. The latter, on the other hand, seems to be rather low in view of the relative intensities of the strongest diffraction lines of the two phases. It appears that the work of Itagaki *et al.* [19] is a more accurate description of the αAl lattice parameter-solubility extension relationship in Al–Si alloys, yielding a value of 6.35 at % Si.

It should also be noted that the relative intensities of the αAl diffraction lines match perfectly well with those listed in powder diffraction files. The same is true also for Si, indicating that both αAl and Si are randomly oriented.

A fine and homogeneous cellular structure is revealed on the cross-section of as-quenched ribbons (Fig. 3). Fig. 4a is a TEM micrograph of this structure taken in the plane of the ribbon. At still higher magnifications, very fine Si particles can be identified. These particles, approximately 20 nm in diameter, are distributed inside the αAl cells and also gather at cell boundaries (Fig. 4b). It seems reasonable to infer from this micrograph that some Si precipitation might have taken place during post-solidification cooling. The selected area diffraction patterns (SADPs) from the interior of the cells show spotty rings of randomly oriented Si particles and the individual reflections of the αAl matrix (Fig. 4c). The average cell size is less than 0.5 μm. Hence, the emprical relation proposed by Matyja *et al.* [21] for an Al–11 at % Si alloy

$$q = (47/d)^3$$

where d is the characteristic size of the microstructure in μm, yields a cooling rate, q, on the order of 10^6 K s^{-1}, typical of the PFC process.

The scale of the microstructure was found to be uniform across the thickness as well as along the width of the ribbons. Electron microprobe analysis showed no detectable segregation patterns. Unlike some earlier studies which report structurally and morphologically different regions in melt-spun ribbons and splats of Al–Si alloys [11, 14, 16], no transition

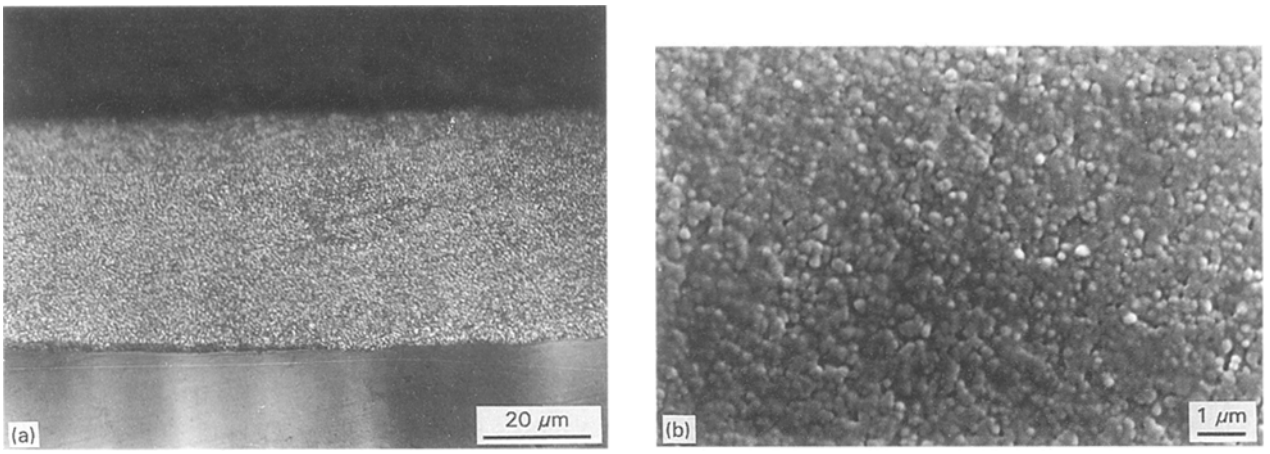

Figure 3 (a) Optical and (b) SEM micrographs revealing the microstructure on the cross-section of as-quenched ribbon.

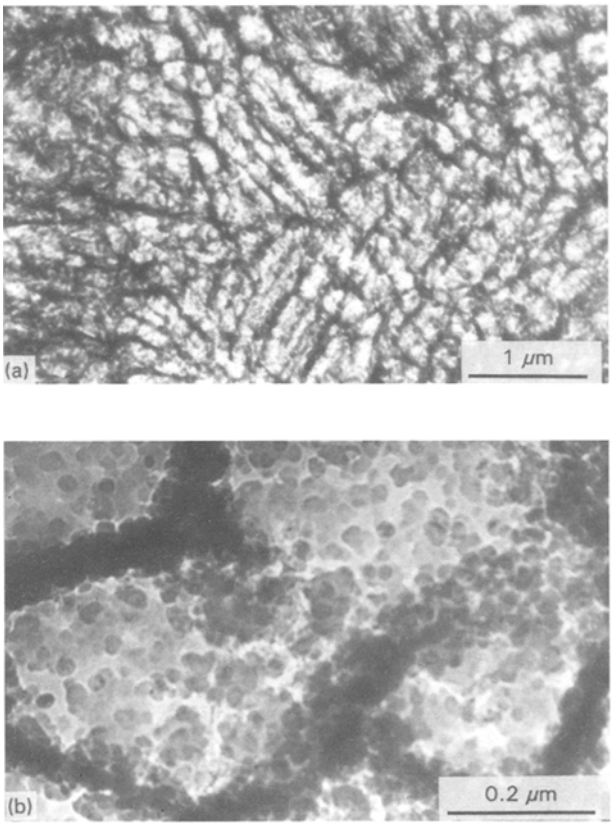

Figure 4 (a,b) Bright-field micrographs revealing a cellular structure and (c) SADP of the intra-cellular region.

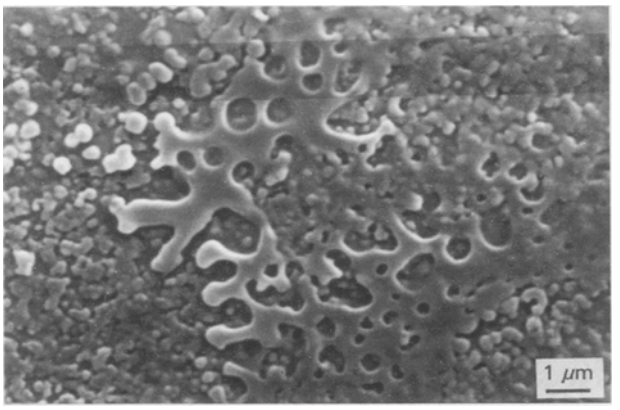

Figure 5 SEM micrograph of a dendritic region.

from cellular to dendritic structure was observed. Available experimental data suggests that the multi-zone structures are generally associated with thicker ribbons [14]. Undercooling at the solidification front, which is suppressed due to recalescence, cannot afford a cellular mode of solidification anymore, at some point away from the substrate when the section is rather thick.

Although cellular solidification was identified as the dominant mechanism, a few dendritic regions were also spotted (Fig. 5). Heterogeneities, rather than general recalescence, are believed to be responsible for such local variations. Impurities might act as heterogeneous nucleation sites and interfere with the solidification behaviour by reducing the undercooling achieved prior to solidification.

A common microstructural aspect of rapidly solidified aluminium alloys is a featureless zone along the wheel-side of cross-section where the cooling rate reaches a maximum [13, 14, 16, 21]. This zone, often referred to as zone A following the work of Jones [23], appears white since it does not respond to etching favourably. Such a zone was observed discontinuously existing only in certain regions which are substantially thinner than the average ribbon (Fig. 6). The featureless zone is separated from the cellular region by a sharp interface and its width appears to be inversely

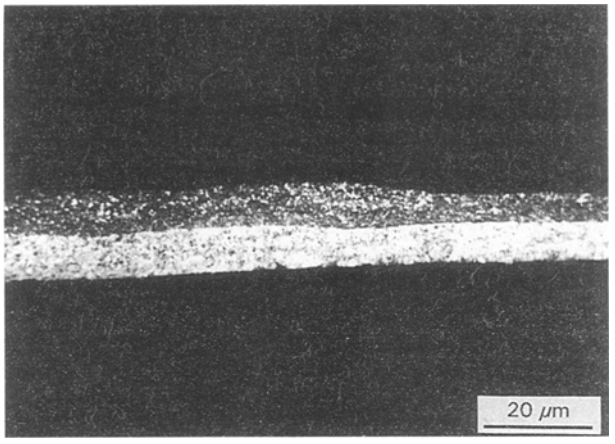

Figure 6 Optical micrograph revealing the featureless zone along the wheel-side.

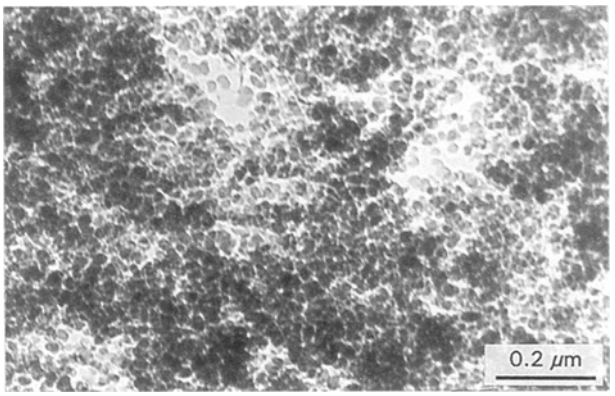

Figure 7 TEM micrograph of the featureless zone.

proportional to the cross-sectional thickness. No featureless zone could be identified, however, in sections thicker than 30 μm, suggesting the existence of a critical cooling rate for its formation. This critical cooling rate is apparently higher than 10^6 K s^{-1} which yields a single-zone cellular structure in a 45 μm thick ribbon.

Fig. 7 is a TEM micrograph taken from the wheel-side of a thin section, showing a fine distribution of discrete Si crystals. It is difficult to resolve the cellular morphology in this micrograph, possibly because of a very fine cell spacing which is of the same order with the Si particle size. It is well established that zone A of rapidly solidified Al alloys has a microcellular structure [24]. A cell size of 20–50 nm was reported for zone A of an Al–Fe alloy [25].

The featureless zone is known to be associated with a very rapidly moving solidification front, as in thinner sections, which reduces partitioning and leads to extensive solute trapping. The increased chemical homogeneity, thus obtained, accounts for the lack of etching on the wheel-side of thin ribbons.

4. Conclusions

Ribbons of an Al–12 wt % Si alloy produced by quenching from the melt at a cooling rate of 10^6 K s^{-1} have undergone cellular solidification with no transition to a dendritic structure. The single-zone structure suggests that undercooling at the solidification front was large enough to compensate for recalescence, thus avoiding such a transition in the solidification behaviour.

XRD analysis of as-quenched ribbons revealed two phases: (i) a supersaturated aluminium solid solution and (ii) Si, both of which are randomly oriented. Aluminium solid solution forms the cellular structure and the latter consists of nanosize particles which are distributed inside αAl cells and also gather at cell boundaries. These ribbons, generally of uniform thickness in the 40–50 μm range, are structurally and chemically homogeneous as evidenced by light, electron microscopy and XRD work.

Thinner sections which have apparently experienced substantially higher cooling rates show, in addition to a cellular structure, a featureless zone along the wheel-side of the ribbon. TEM micrographs of this zone reveal a fine distribution of discrete Si crystals and a microcellular αAl structure.

Acknowledgements

The author is indebted to Z. Misirli, N. Parkan, O. Arisoy and O. Ipek for their help in the experimental part of this work. Financial support of The Scientific and Technical Research Council of Turkey is gratefully acknowledged.

References

1. M. COHEN, B. H. KEAR and R. MEHRABIAN, in "Rapid Solidification Processing: Principles and Technologies", edited by R. Mehrabian, B. H. Kear and M. Cohen (Claitor's, Baton Rouge, 1980) p. 1.
2. N. J. GRANT, in "Rapidly Quenched Metals", edited by S. Steeb and H. Warlimont (North Holland, Amsterdam, 1985) p. 3.
3. F. H. FROES, Y. W. KIM and F. HEHMANN, *J. Metals* **39** (1987) 14.
4. H. JONES, *Aluminium* **54** (1978) 274.
5. E. J. LAVERNIA, J. D. AYERS and T. S. SRIVATSAN, *Int. Mater. Rev.* **37** (1992) 1.
6. W. G. J. BUNK, *Mater. Sci. Engng* **134A** (1991) 1087.
7. S. K. DAS and L. A. DAVIS, *ibid.* **98** (1988) 1.
8. S. K. BOSE and R. KUMAR, *J. Mater. Sci.* **8** (1973) 1795.
9. A. BENDIJK, R. DELHEZ, L. KATGERMAN, Th. H. De KEIJSER, E. J. MITTEMEIJER and N. M. van DER PERS, *ibid.* **15** (1980) 2803.
10. R. DELHEZ, Th. H. De KEIJSER, E. J. MITTEMEIJER, P. van MOURIK, N. M. van DER PERS, L. KATGERMAN and W. E. ZALM, *ibid.* **17** (1982) 2887.
11. J. A. van DER HOEVEN, P. VAN MOURIK and E. J. MITTEMEIJER, *J. Mater. Sci. Lett.* **2** (1983) 158.
12. M. van ROOYEN, N. M. van DER PERS, L. KATGERMAN, Th. H. De KEIJSE and E. J. MITTEMEIJER, in "Rapidly Quenched Metals", edited by S. Steeb and H. Warlimont (North Holland, Amsterdam, 1985) p. 823.
13. S. PAIDASSI and J. CHEVRIER, *ibid.* p. 957.
14. C. ANTONIONE, L. BATTEZZATI and F. MARINO, *J. Mater. Sci. Lett.* **5** (1986) 586.
15. N. APAYDIN and R. W. SMITH, *Mater. Sci. Engng* **98** (1988) 149.
16. P. TODESCHINI, G. CHAMPIER and F. H. SAMUEL, *J. Mater. Sci.* **27** (1992) 3539.
17. J. YEH and C. TSAU, *Met. Trans.* **23A** (1992) 2313.

18. A. M. BASTAWROS and M. Z. SAID, *J. Mater. Sci.* **29** (1993) 1143.
19. M. ITAGAKI, B. C. GIESSEN and N. J. GRANT, *Trans. ASM* **61** (1968) 330.
20. P. H. SHINGU, K. B. KOBAYASHI, K. SHIMOMURA and R. J. OZAKI, *J. Jpn. Inst. Met.* **37** (1993) 433.
21. H. MATYJA, B. C. GIESSEN and N. J. GRANT, *J. Inst. Metals* **96** (1968) 30.
22. V. K. VASUDEVAN, H. L. FRASER. *Mater. Sci. Engng* **98** (1988) 213.
23. H. JONES, *ibid.* **5** (1969–1970) 1.
24. L. A. BENDERSKY, M. J. KAUFMAN, W. B. BOETTINGER and F. S. BIANCANIELLO, *ibid.* **98** (1988) 213.
25. G. VIGIER, U. ORTIZ-MENDEZ, P. MERLE, G. THOLLET and F. FOUQUET, *ibid.* **98** (1988) 191.

Received 23 September 1994
and accepted 4 October 1995